Corrugated shells: an algorithm for generating double-curvature geometric surfaces for structural analysis

M. Lai[a,b,*], S. R. Eugster[b], E. Reccia[a], M. Spagnuolo[a], A. Cazzani[a]

[a] *Dipartimento di Ingegneria Civile Ambientale e Architettura, Università degli Studi di Cagliari, Cagliari, Italy*
[b] *Institute for Nonlinear Mechanics, University of Stuttgart, Stuttgart, Germany*

Abstract

Analysis of corrugated shell structures is an interesting problem in Structural Mechanics, which has many practical applications in Civil Engineering and Architecture. Thanks to corrugation, these structures have a remarkable feature: the wavy (undulated) shape in their edge provides significant enhancements in their structural behaviour, increasing the bending stiffness at the edge and allowing for a non-negligible reduction of its thickness. Moreover, looking at the non-linear behaviour, domes corrugation plays a relevant role in instability phenomena, such as the influence of imperfections and increasing resistance to snap-through.

A problem in the study of such kind of shells is the definition of mathematical and geometrical model and the construction of a suitable mesh to perform FE analyses. The aim of this paper is to find an automated way to generate a double-curvature geometric surface that can be used both in

*Corresponding author
Email address: matteolai@unica.it (M. Lai)

static and in non-linear stability analyses of such corrugated shell structures. A method to generate a NURBS surface, suitable for a parametric FE analysis from a geometrical model expressed in a parametric form, is proposed and applied to a shell inspired by the well-known dome designed by Pier Luigi Nervi in 1959 for the roof of the Palasport Flaminio in Rome.
Keywords: corrugated shells, shallow shells, domes, Palasport Flaminio, Pier Luigi Nervi

1. Introduction

The problem presented in this work concerns the structural analysis of corrugated shell structures. These structures have a remarkable characteristic: the wavy shape of their edge gives a significant improvement to their structural behaviour, increasing the bending stiffness at the edge, thus allowing the designer to reduce its thickness. A problem in studying this structural typology is how to deal with its complex geometry. This paper aims to find an automated way to generate a double-curvature geometric surface, given its mathematical description, which can be used both in static and non-linear stability analyses of corrugated shell structures.

For properly treating this topic, it is useful to recall a state-of-the-art where the problem studied in the present work can be framed. Some relevant examples in the field of corrugated shell structures can be found along the history of Civil Engineering. In East Anglia (England) from XVII until XIX century wavy fences were largely built as garden walls, known as *Crinckle crankle walls* (see Fig. 1). Some of them still exist in Suffolk and Hampshire. This kind of construction, which has been attributed to Dutch engineers [1], presents a wavy shape that provides the wall with bending stiffness and improves its structural response to horizontal loads. As a consequence, bricklayers could build a slender wall made of a single line of bricks without the need for abutments or buttresses. The effect of corrugation, then, is to improve the mechanical behaviour of this structure. The same remark will also be true for shells, as it will be clear in the following. Specifically, one can observe corrugation in seashell structures arising as a result of optimization processes.

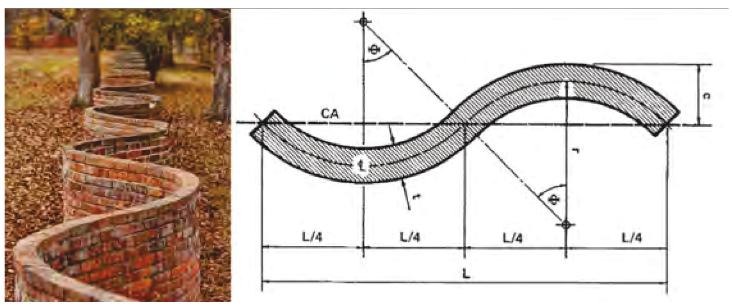

Figure 1: A Crinkle Crankle wall in Suffolk (UK), left. A sketch of the same wall, right.

Indeed, corrugated shells can be found in nature: structures of such type can be obtained by a topologic optimization process, as those occurring in bone reconstruction (see, for example, [2–4]). A relevant example, also of interest for the topic of the present work, is represented by seashells. It is observed that the mussel minimizes the effort in building its dwelling changing from a smooth to a corrugated shape [5]. The outcome of the new smart shape is to increase the mechanical resistance with the same amount of material. As a consequence, the optimized structure is said to be shape-resistant. The study presented herein is motivated by similar considerations related to efficiency and resistance criteria.

On the Civil Engineering side, the need for corrugated shells or plates is also motivated by structural efficiency. The main differences between the Civil Engineering case and other fields (such as the cited example of seashells) consist in scale and, clearly, in the employed materials. Generally in Civil Engineering and Architecture a standard material is reinforced concrete (shortly, RC), whose high-performance dissipation properties are also known, as it was pointed out in [6–8]. In addition, special attention should be given to the durability of this material, [9–11].

RC has always been an excellent material to be used in optimized [11], [12] and customized-shaped building [13], also in the Italian school of Structural Engineers, which between the '50s and '70s was led by Pier Luigi Nervi and Sergio Musmeci. An outstanding piece of Italian architecture, where a corrugated shell made of reinforced concrete is used, is the roof of a gasoline station in Sesto San Giovanni (Milano), designed by Aldo Favini in 1949, which was unfortunately destroyed some years later. Then this type of construction has been progressively fallen into disuse, due to the increase in the cost of the formwork and scaffolding.

As it has been already remarked, some models can be suitably adapted to apparently different structures. Referring to Fig. 2, one can observe different objects where corrugation has a relevant role: potentially the spirit of the present work is to develop an algorithm which is useful for all these cases, independently on the scale or material. An extensive body of literature exists and deals with the connection between form and structure, and these topics are covered in foremost books like [14, 15]. A new gaze is provided from the SIXXI project, whose purpose is to give a distinct point of view on the Italian school of Structural Engineering, and is set out in [16]. Even though primary source can be found in Nervi's book [17], some recent advancements have been provided in [18, 19]. The inspiration for this work has been taken from one of Nervi's works: the shallow shell designed for Rome Olympics game in 1960 to cover the roof of the Palazzetto dello Sport or, shortly, *Palasport Flaminio* (from the name of the district of Rome where it was built and still stands nowadays).

Figure 2: Example of corrugated shells: (a) Nervi's Palasport Flaminio dome, (b) Hobermann deployable structure, (c) Favini's roof, (d) corrugated sea-shells.

Nervi's shell is a foremost piece of unique architecture and it also constitutes an inexhaustible source for structural design, even in different fields. For instance, it has been a source of influence for the Iris Dome retractable roof, which was designed by Charles Hobermann [20]. This kind of corrugated shapes, known as *umbrella-type surfaces*, can be studied from a mathematical point of view as it has been done, in a more general framework, in [21].

One can employ a representation of 2-D surfaces in Cartesian coordinates depending on a set of parameters defined in a closed interval. A comprehensive guide for a wide variety of parametric equations can be found in [22].

From a Structural Mechanics point of view, the consequences of corrugations in building structures have not yet been entirely investigated, perhaps due to the intrinsic difficulties to manage the mathematical implications of corrugation. Some theoretical background is given for static analyses in [23] and considerations about the stability and multi-stability of open corrugated shell are pointed out in [24]. In [25] it is possible to find a parametric analysis devoted to understanding the role of corrugation in improving the seismic resistance of vaults and domes.

In [26–29] some relevant results in the field of shells were set out. These studies can be useful also for generalizing the results presented in this work [30–34].

Frequently, in Architecture it is needed to design large-span roofs: to this aim, the theory of shells provides the most effective approach, introducing structural problems that need to be properly taken into account. A remarkable problem consists in enhancing the structural resistance. This can be made in different ways, as, for instance, by increasing the thickness of the shell surface or by placing a ring-beam on the shell edge. In this context a smarter solution (also from an architectural and aesthetics point of view) consists in employing corrugated shell surfaces which allow in reducing the shell thickness.

The above recalled literature is necessary to address the main aim of this paper: to recognise the influence of corrugations in the mechanics of shells, taking into account relevant non-linear effects affecting slender and shallow shells, whose edge is wavy-corrugated. Non-linear behaviour remarkably affects the shell mechanical performances, such as snap-through mechanism and buckling instability phenomena [35–42]. A successfully employed method in dealing with this kind of problem consists in using a set of safety factors to knock down the theoretical results: see for example the NASA aeronautics recommendations [43].

The first step for performing a correct numerical analysis is to set a procedure which can produce geometrical objects replicating the mathematical dome shape in a process suitable for structural analysis using doubly-curved elements. In Section 2 the geometrical representation of a corrugated shell is introduced in such a way that mathematical parametric equations are given. In Section 3 an algorithm to represent a NURBS based surface is presented. Numerical results are shown and discussed in Section 4 in order to investigate the influence of shell corrugation. Finally, in Section 5, some concluding remarks are presented.

2. Wavy-edge shell parametric description

In this section, a mathematical description of a wavy-edge surface inspired to the Nervi's Palasport Flaminio dome is proposed. Its equations depend on several parameters which control the corrugation shape along the shell side.

The adopted spherical polar reference system is shown in Fig. 3, where r is the radial distance from the pole, ϑ is the colatitude angle (the complement to the latitude angle) and φ is the longitude angle. So, a generic point P, belonging to the 3-D space, is uniquely identified by its spherical coordinates (r, ϑ, φ). A parametric representation of a wavy-edge spherical shell can be given introducing a parametrization of its radius. A surface could thus be described by using two parameters only, viz. ϑ and φ, where each pair (ϑ_i, φ_i) describes a point P_i which belongs to the surface.

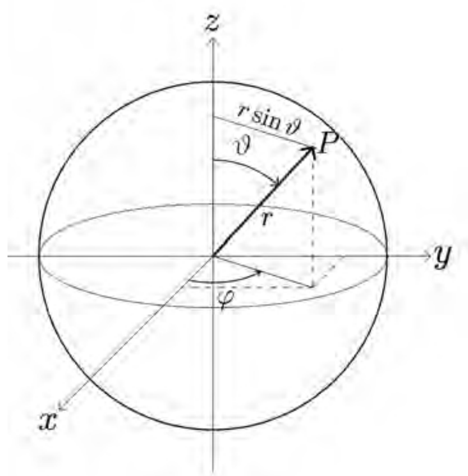

Figure 3: Spherical polar coordinate system.

Considering a perfect spherical shell, whose radius is R_0, its *parametric equations* are the classical ones

$$\begin{cases} x = R_0 \sin\vartheta \cos\varphi \\ y = R_0 \sin\vartheta \sin\varphi \\ z = R_0 \cos\vartheta. \end{cases} \tag{1}$$

From Eq. (1), by squaring and summing up (term by term) both sides, parameters ϑ and φ can be eliminated and the resulting *implicit* representation of the spherical surface is obtained:

$$x^2 + y^2 + z^2 - R_0^2 = 0. \tag{2}$$

Now, recalling that the radial distance r from the pole is given, in terms of Cartesian coordinates, by:

$$r = \sqrt{x^2 + y^2 + z^2},$$

an *explicit* representation of the spherical surface results:

$$r = R_0. \tag{3}$$

Looking at Eq. (3) it is apparent that in the case of a sphere the radial distance of any point of the surface is independent of the spherical coordinates ϑ, φ. This consideration suggests an easy way to construct a surface, shaped as a portion of a hemispherical shell but exhibiting a corrugation on the edge. Indeed such corrugated edge can be treated as a perturbation of the constant radius R_0, resulting in a wavy-edge. Then, for such surface the radius $r = r(\vartheta, \varphi)$ may be represented as

$$r = R_0 \left[1 + f(\vartheta) g(\varphi)\right]. \tag{4}$$

In Eq. (4) the perturbation is made up by two factors: the former $f(\vartheta)$, depends only on colatitude ϑ and gives the shape of the perturbed meridian, while the latter $g(\varphi)$ depends only on the longitude angle φ and modulates the form of all parallels. In order to get a cyclic symmetry along each parallel line, function $g(\varphi)$ must be periodic; a suitable choice to get a smooth repetition by a whole number n of a basic wave pattern is then:

$$g(\varphi) = \cos(n\,\varphi). \tag{5}$$

This ensures that an undulated wave is repeated n times along the surface edge, i.e. the period of function g is simply $2\pi/n$; in order to obtain that the fundamental (or *zero*) meridian $\varphi = 0$ is indeed perturbed with reference to the spherical shape, the cosine function has been preferred to its sine counterpart.

Function $f(\vartheta)$, which controls the perturbation of the radius along the meridian with reference to that of a perfect sphere, R_0, can be chosen in several ways. A possible choice is:

$$f(\vartheta) = aH(\vartheta - \vartheta_0)\left(\frac{\vartheta - \vartheta_0}{\vartheta_0}\right)^2. \tag{6}$$

In Eq. (6) a is a parameter controlling the amplitude of the perturbation, H is Heaviside step function (or unit step function), defined as:

$$H(\vartheta - \vartheta_0) = \begin{cases} 1, & \text{if} \quad \vartheta \geq \vartheta_0 \\ 0, & \text{if} \quad \vartheta < \vartheta_0, \end{cases}$$

whose role is to switch on the radius perturbation in correspondence of ϑ_0, namely the colatitude angle at which such perturbation originates. Finally the term $(\vartheta - \vartheta_0)^2/\vartheta_0^2$ has been introduced to produce a smooth variation of r along the meridian in a neighborhood of ϑ_0. Despite the presence of Heaviside's step function, it comes out from Eq. (6) that the resulting radius $r(\vartheta, \varphi)$ is an almost everywhere continuous and differentiable function of its arguments.

If a smoother shape is desired, the unit step function H can be replaced by a continuously differentiable function approximating it, like, for instance, the hyperbolic tangent; consequently, in this case, $f(\vartheta)$ can be expressed by:

$$f(\vartheta) = \frac{a}{2}\left[1 + \tanh(b(\vartheta - \vartheta_0))\right], \tag{7}$$

where a is again a parameter controlling the amplitude of the perturbation, while b is a second parameter which, when increases, makes steeper the graph of the function and allows approximating, with the desired accuracy, a step function with a continuous one. Besides, one should notice that the value of the derivative at $\vartheta = \vartheta_0$ differs for the two proposed parametrizations: for Eq. (6) such value is zero, whereas for Eq. (7) this is not the case.

A mathematical representation of the corrugated surface is then given by updating the previously mentioned equations of a hemispherical shell, using $r(\vartheta, \varphi)$ defined by Eq. (4) instead of the constant radius R_0. As a consequence, the parametric equations of the corrugated surface become:

$$\begin{cases} x = r(\vartheta, \varphi)\sin\vartheta\cos\varphi \\ y = r(\vartheta, \varphi)\sin\vartheta\sin\varphi \\ z = r(\vartheta, \varphi)\cos\vartheta. \end{cases} \tag{8}$$

The difference between the two possible choices which were presented above is shown in Fig. 4. For the case described by Eq. (6), the following parameters have been adopted: $\vartheta_0 = \pi/6$, $a = \vartheta_0^2$; for that represented by Eq. (7) $\vartheta_0 = \pi/6$, $a = 1/50$, $b = 50$. In both cases $g(\varphi)$ has been defined as in Eq. (5) where a value $n = 36$ has been assumed; for comparison purposes the opening of the dome has been fixed in both cases to the value $\vartheta_f = \pi/5$. A magnified portion of the corrugated edge is shown for both cases in Fig. 5.

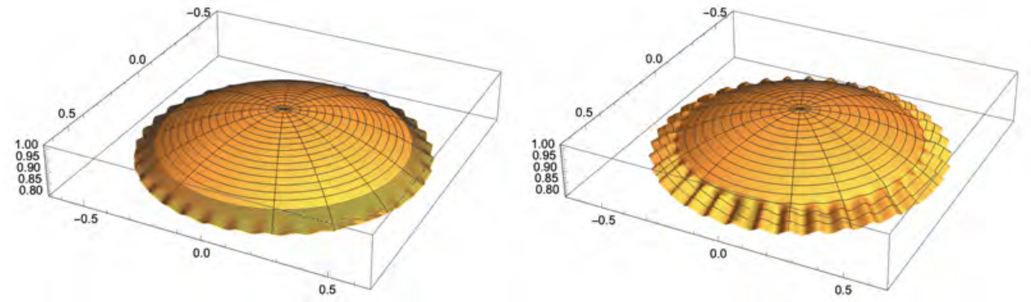

Figure 4: Corrugated surface produced by two possible choices of the perturbation function $f(\vartheta)$: unit step function, Eq. (6) (left) and hyperbolic tangent, Eq. (7) (right). In both cases the same opening of the dome ϑ_f and unperturbed radius R_0 have been assumed.

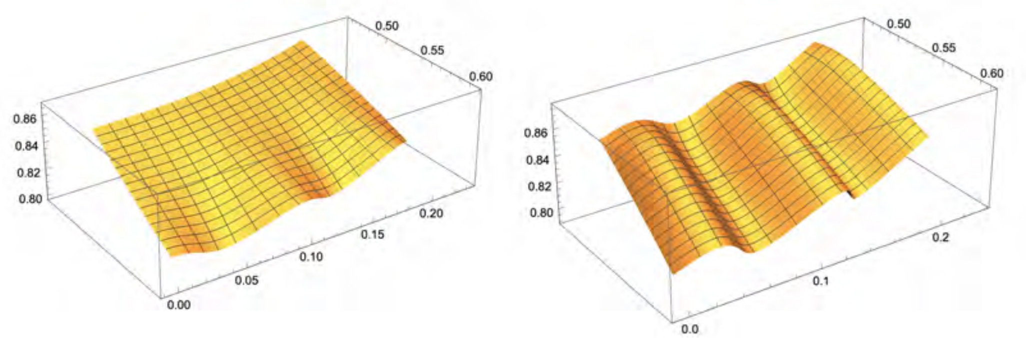

Figure 5: Magnified portion of the corrugated edge for the two cases presented in Eq. (6) (left) and Eq. (7) (right).

3. Generating a suitable geometry for FE computations

Starting from the above introduced parametric description of the corrugated shell surface, it is now possible to generate a geometry which is suitable for the subsequent either linear or non-linear analyses. Of course to this aim, geometry formulation must be accurate. Indeed, in non-linear analyses any imperfection would result in a sudden reduction of the critical load. It is common to introduce slight imperfections (related to the geometry) to trigger an equilibrium path bifurcation in large-displacement or buckling analyses [44–48]. Now, a standard procedure to create a geometric model adopts usually a flat-faceted surface generated by CAD software. This does not guarantee that geometrical accuracy can be achieved in subsequent computations. A better option consists in using computational tools such as Non Uniform Rational Basis Spline functions (henceforth, NURBS) to model the surface. To conceive a geometric object, the following steps must be followed. As a basic criterion, given the cyclic symmetry of the surface, only a piece of surface must be generated, for instance (in the present case) one of the slices lying between two subsequent supports has been drawn. In Nervi's dome, there are 36 supports and each such slice spans exactly 10°. The procedure for generating the geometry, which is described in Fig. 6, can be summarized as follows:

i. A code has been developed in a geometric modelling software, whose aim is to use the parametric equation of the surface to numerically compute a satisfactory set of coordinate pairs (ϑ_i, φ_i). The dimension set depends on the specified number of points along the colatitude and longitude direction. A cross-reference algorithm is employed to create a pair (ϑ_i, φ_i), representing a single point belonging to the surface. Therefore, a numerical algorithm (available on the software library), employing NURBS, is applied to the points set which should better approximate the shape of the geometric object. The accuracy of the

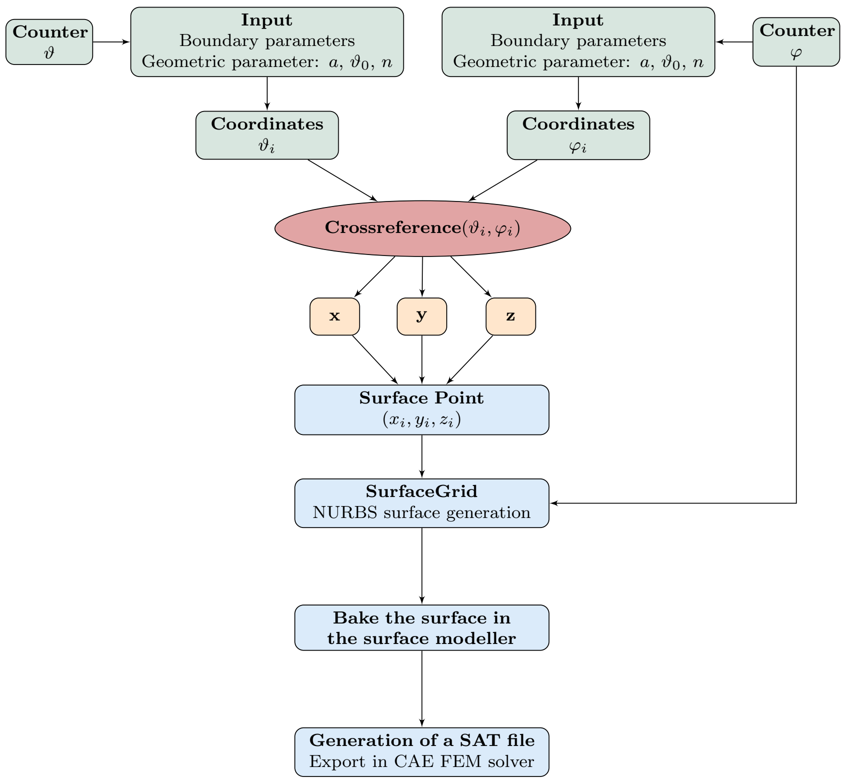

Figure 6: Block-diagram of surface generating algorithm.

representation depends on the initial user choice. Nevertheless, it is clear that the accuracy in generating the surface depends on the chosen number of points;

ii. The algorithm outcome is then graphically visualized in the surface modeler. To produce the obtained NURBS surface, it is necessary to bake it into the graphical interface;

iii. The surface is exported into a convenient file exchange format, such as the ACIS format. This file includes complete pieces of information about the geometry and can be imported into an advanced FEM solver;

iv. The ACIS file is imported into the CAE FEM solver and constitutes a single portion of the surface, see Fig. 7. Inside the pre-processor, the portion is suitably reflected and then a circular pattern is implemented around the z-axis to generate the whole dome. All these slices need then to be merged into a single object.

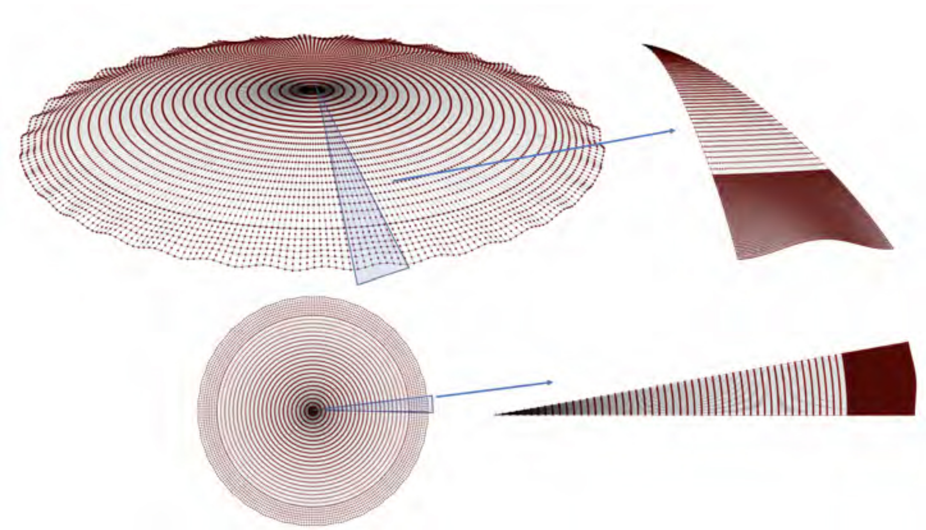

Figure 7: The automatically generated set of points for the model of Nervi's dome of Palasport Flaminio.

The obtained part can then be meshed inside the FE pre-processor. It is requested that even the mesh closely reproduces the shape without deforming the geometry. As a consequence, the chosen type of finite element should be able to reproduce a conveniently small portion of double-curvature surface such as an eight-noded shell element with six or five degrees of freedom, and where that is not possible (e.g. in the dome apex) to six-noded triangular elements with five degrees of freedom. In addition, this kind of elements is suitable to perform buckling analysis. However, to obtain a regular mesh, a sweep algorithm has been used for getting a mesh made of quadrilateral elements, whose edges are aligned with meridians and parallels. The resulting mesh shows however a main drawback: indeed, the elements which are close to the vertex turn out to be severely distorted. In order to overcome such problem, a minute partition is applied near the apex. Hence, in this region a single six-noded triangular element is employed for each slice.

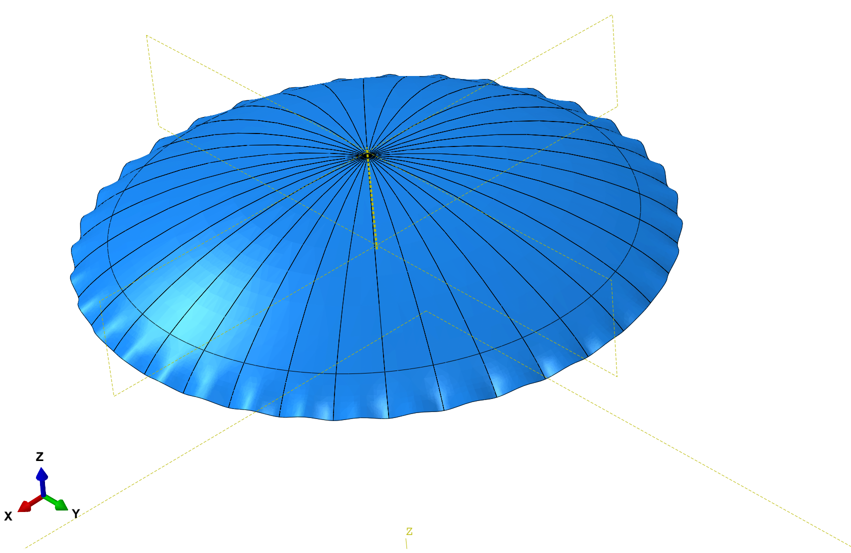

Figure 8: Resulting assembly of the slices of the model of Palasport Flaminio dome.

4. Geometrical and mechanical data

The analysis of a shell inspired by RC Palasport Flaminio dome designed by Nervi has been accomplished. In this section the geometrical and mechan-

Table 1: Geometric properties of the Palasport Flaminio dome

Radius	R_0	51.039 m
Roof span	L	60.000 m
Shell thickness	t	0.200 m
Opening angle	ϑ_f	$\pi/5$ rad
Angle where perturbation starts	ϑ_0	$\pi/6$ rad
Wave number	n	36

ical assumptions adopted for such RC shell are summarized. Original design blueprints are available in the MAXXI (the Art Museum of the XXI century) archives in Rome. Besides, the span and the opening angle are given in [18], as reliable average measurements. All these data are presented in Table 1. In particular, a sketch of the geometry is provided in Fig. 9.

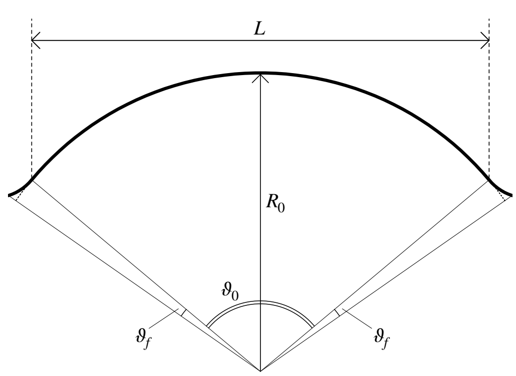

Figure 9: Schematic representation of the shell geometry.

In [49] a different opening angle has been considered, which, however, does not seem to agree with the architectural blueprints reported in [18]. Instead mechanical characterization of the material has been simplified as follows:

i. Only the linear part of the stress-strain curve is taken into account. So, plasticity and other kind of non-linear behaviour have been disregarded;

ii. RC is always assumed to be uncracked;

iii. Time dependent effects on material properties are completely neglected, and Young's modulus E is assumed to be equal to 30 GPa;

iv. Poisson's coefficient ν is similarly assumed to be constant and equal to 0.2;

v. Concrete strength class is required to be C20/C25 (Eurocode classification), whose density is 2500 $\mathrm{kg/m^3}$. Even though Nervi's dome is a RC shell with stiffeners, which follow a certain spherical path, it is reasonable to assume that shell thickness is constant and equal to 0.2 m.

For a more accurate survey about mechanical properties of concrete, partially based on tested specimens and survey, even though they are referred to a nearby canopy which was realised by the same Nervi (Stadium Flaminio) a reader may rely on [50].

In the mentioned reference, particular emphasis has been placed on the differences between *ferrocemento*, the building material adopted by Nervi, and the standard RC.

5. Analysis

It is now possible to carry out a statical analysis of the structure by using computational methods. For the sake of simplicity, only the shape produced by Eqs. (4), (5) and (6) has been considered.

The load-case consists of a uniform external normal pressure q_0 applied inwards to the whole surface, whose magnitude is 5 kPa. Since the extension of the shell is such that its rise over span ratio makes it rather shallow, it is possible to approximate the self-weight load condition with a uniform pressure. This approximation allows tackling the problem of stability of edge-corrugated shells in an easier framework. To understand the effect of edge-corrugation, a comparison between a shell with the same geometrical measure but without corrugation is shown.

The structure has been envisioned to behave according to the classical membrane theory. In agreement with this theory, supports should restrain motion only along the tangent direction. According to that, the dome edge requires to be simply supported, so that edge rotation and out-of-plane surface extension/shrinking are allowed. Therefore, the designer put all his efforts to guarantee that no edge disturbances occur. As a matter of fact, the pillar inclination follows the tangent to the boundary surface. Nevertheless, the edge is fully restrained on the support and free between the supports. If other constraints are applied, the membrane state will be supplemented by bending and twisting effects. As a consequence, such supplementary effects should be taken into account.

In terms of the membrane stress resultants N_ϑ, N_φ and $N_{\vartheta\varphi} = N_{\varphi\vartheta}$, which are, respectively, the in-plane normal components of stress directed along the

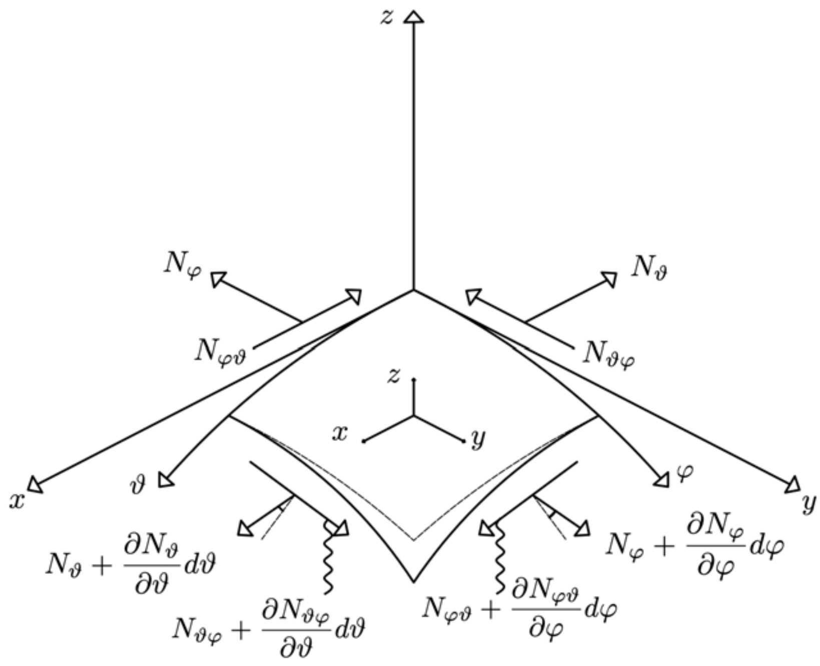

Figure 10: Equilibrium of a differential element of a shell with membrane stress-resultants.

meridian line and the parallel line, and the in plane shear stress components (see Fig. 10), the fundamental differential equations of equilibrium in the membrane theory of shells, written with reference to the lines of curvature on the middle-surface are given by [51] and read:

$$
\begin{aligned}
&\frac{\partial}{\partial \vartheta}(BN_\vartheta) - \frac{\partial B}{\partial \vartheta} N_\varphi + \frac{1}{A}\frac{\partial}{\partial \varphi}(A^2 N_{\vartheta\varphi}) + ABX = 0 \\
&\frac{\partial}{\partial \varphi}(AN_\varphi) - \frac{\partial A}{\partial \varphi} N_\vartheta + \frac{1}{B}\frac{\partial}{\partial \vartheta}(B^2 N_{\vartheta\varphi}) + ABY = 0 \\
&\frac{N_\vartheta}{R_1} + \frac{N_\varphi}{R_2} - Z = 0.
\end{aligned} \tag{9}
$$

In Eq. (9) A and B are the coefficients of the first fundamental form, which gives the squared length of a line element as:

$$ds^2 = A^2 d\vartheta^2 + B^2 d\varphi^2;$$

R_1 and R_2 are, respectively, the curvature radii along the meridian (ϑ-line) and perpendicularly to it; X and Y are external surface loads (i.e. loads per unit area) acting towards increasing values of ϑ and φ, while Z denotes the intensity of surface load per unit area acting along the outward normal.

So, for a perfectly spherical shell, whose radius is R_0, acted upon by a constant external, inward-directed pressure q_0, the previous equations do simplify because $R_1 = R_0$, $R_2 = R_0$, $A = R_0$, $B = R_0 \sin\vartheta$; moreover $X = 0$, $Y = 0$, $Z = -q_0$. Finally for the axial symmetry, it is everywhere $N_{\vartheta\varphi} = 0$ and $N_\vartheta = N_\vartheta(\vartheta)$, $N_\varphi = N_\varphi(\vartheta)$, i.e. they do depend only on colatitude.

The reference solution for a membrane state produced by a uniform pressure load q_0 acting on a hemispherical shell supported along the equator is well-known and can be found, if attention is restricted to some of the major sources only, in [52–54]. Indeed it results:

$$N_\vartheta = N_\varphi = -q_0 \frac{R_0}{2} \tag{10}$$

It should be emphasized that N_ϑ and N_φ, which are given by Eq. (10) and will be used in the sequel as a measure of variance from a perfect membrane state, represent the resultant of the corresponding local stress components σ_ϑ, σ_φ, once they are integrated along the thickness of the shell, t. Important, both theoretical and experimental references about RC shells behaviour can be found in [55–57]. On the other hand, a theoretical solution in terms of Fourier series for a hemispherical shells on discrete supports was set out in [52, 56].

The numerical solutions for the edge-corrugated spherical shells produce local surface stresses, whose general expressions can be computed in terms of the section resultants N_ϑ and N_φ as

$$\sigma_\vartheta = \frac{N_\vartheta}{t}, \qquad \sigma_\varphi = \frac{N_\varphi}{t}.$$

In particular, σ_ϑ is the normal stress acting along the ϑ direction (i.e. that tangent to the meridian) and σ_φ is the normal stress along the φ direction, namely tangent to the parallel.

It should be noticed that, even for the corrugated shell, the above mentioned directions are principal direction of stress for the considered applied load, namely uniform external pressure. All numerical results related to stress are presented in dimensionless form: stress values are indeed divided by the applied external pressure $q_0 = 5$ kPa, while the angular position is given in the dimensionless form ϑ/ϑ_f, where ϑ_f is the colatitude value corresponding to the position of the edge, which is assumed to be the same in all considered cases.

The stresses σ_ϑ and σ_φ along the shell are displayed in the contour plot on the left of Fig. 11 and Fig. 12.

As it is expected, the solution exhibits cyclic symmetry. A comparison with a non-corrugated shell is displayed on the right of Fig. 11 and of Fig. 12.

The stresses corresponding to two meridians, one passing through a support and the other through the crest of a wave will be considered in detail; the output is concisely shown in the graphs that follow.

In particular, Fig. 13 and Fig. 14 show on the left σ_ϑ for the above mentioned meridians, while the stress component σ_φ is shown, for the same meridians,

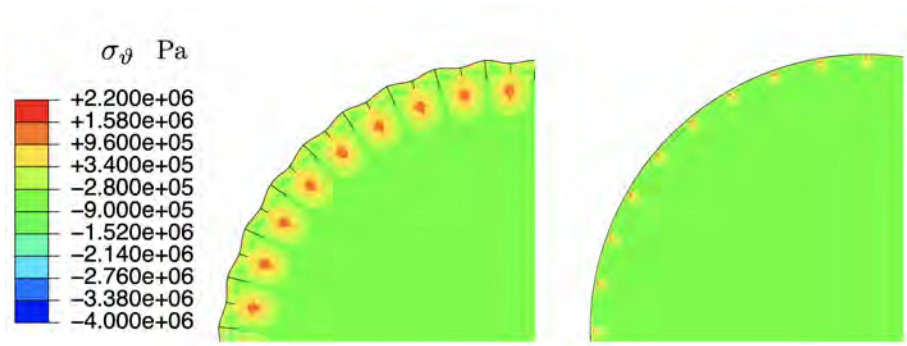

Figure 11: Contour plot of the stress component σ_ϑ for the corrugated-edge dome (left) and for the spherical cap without corrugation (right). In both cases, 36 discrete supports have been considered.

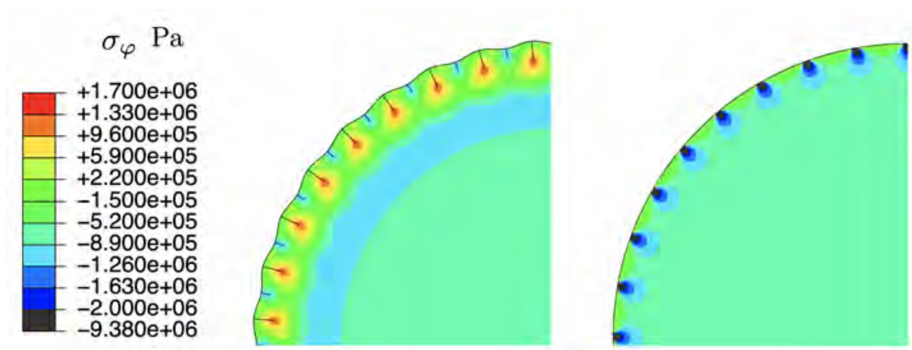

Figure 12: Contour plot of the stress component σ_φ for the corrugated-edge dome (left) and for the spherical cap without corrugation (right). In both cases, 36 discrete supports have been considered.

on the right of the above mentioned Figures.

To understand the reason why in the corrugated shell there is a reduction of stresses, one can usefully look at the bending moment diagrams. Let M_ϑ be the section moment (which is dimensionally expressed as the ratio moment/thickness, thus being homogeneous to a force) along the ϑ direction and M_φ the section moment along the φ direction. Fig. 15 shows the contour

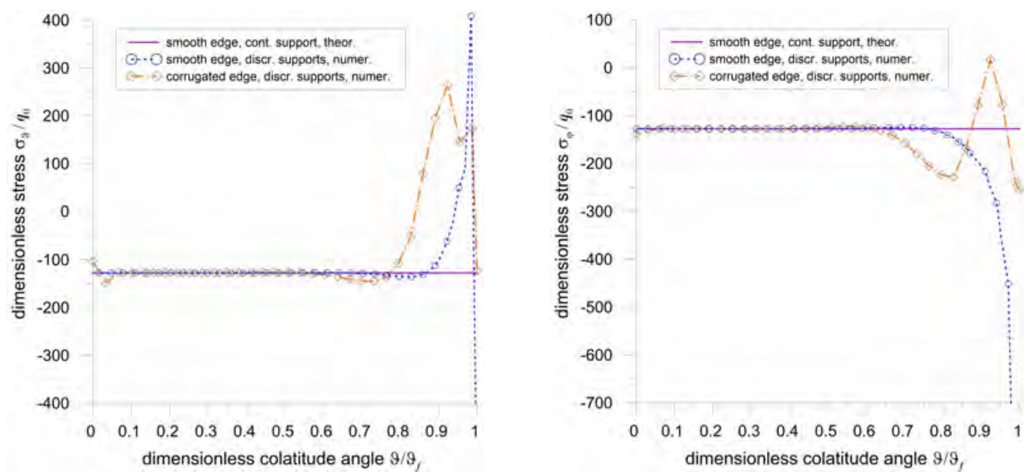

Figure 13: Stress components σ_ϑ and σ_φ along a meridian passing through a support.

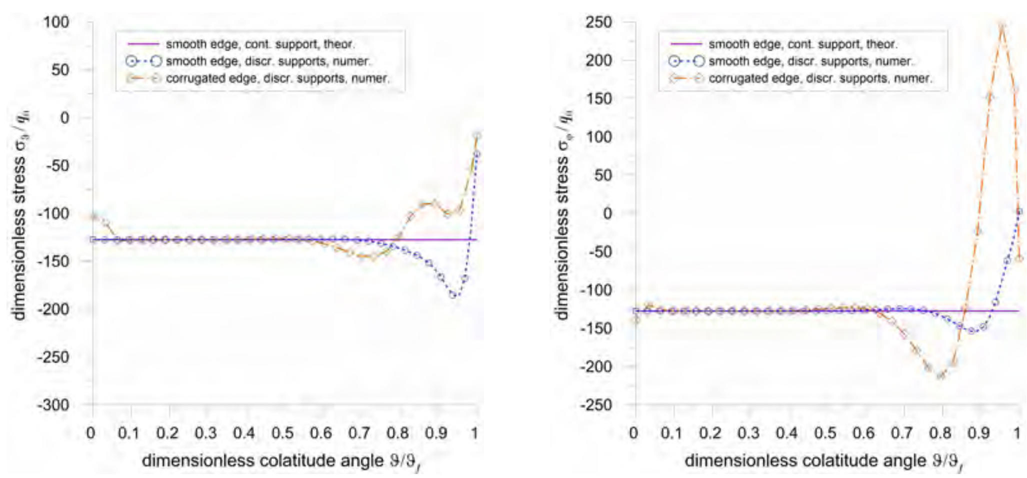

Figure 14: Stress components σ_ϑ and σ_φ along a meridian located between two supports, i.e. corresponding to the crest of the wave.

plot of the section moment M_ϑ for an edge-corrugated (left) and for a non corrugated shell (right).

Similarly, Fig. 16 shows the contour plot of the section moment M_φ for an edge-corrugated (left) and for a non corrugated shell (right).

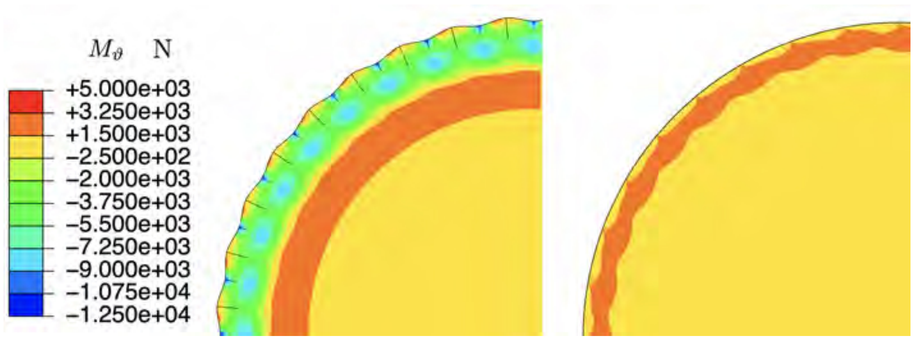

Figure 15: Contour plot of the section moment, M_ϑ for the corrugated-edge dome (left) and for the spherical cap without corrugation (right). In both cases 36 discrete supports have been considered.

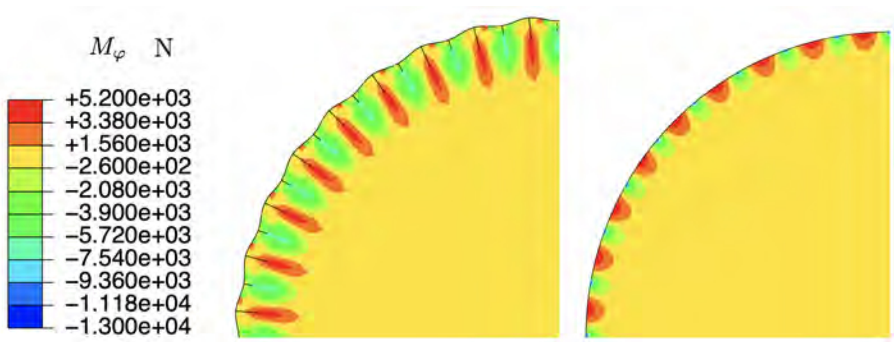

Figure 16: Contour plot of the section moment M_φ for the corrugated-edge dome (left) and for the spherical cap without corrugation (right). In both cases 36 discrete supports have been considered.

The section moments have been plotted for two different meridians, one passing through a support, the other through the crest of the wave. The output is shown in Fig. 17 and 18 in dimensionless form, by dividing the relevant values by the constant $M_0 = 5000$ kN.

M_ϑ (left) and M_φ (right) are plotted in Fig. 17 with reference to the meridian passing through one of the supports; instead the same section moments, in

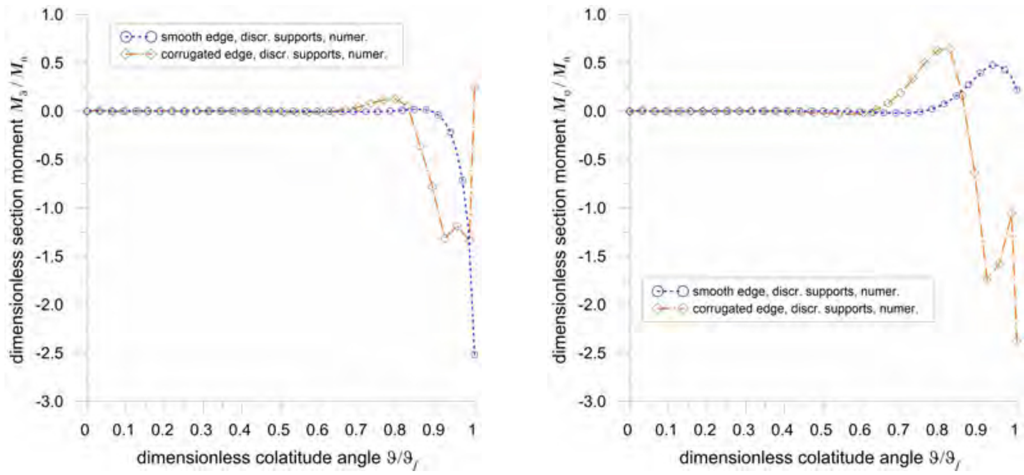

Figure 17: Section moments M_ϑ and M_φ along a meridian passing through a support.

the same order, are plotted in Fig. 18 for a meridian which passes through the crest of the corrugation.

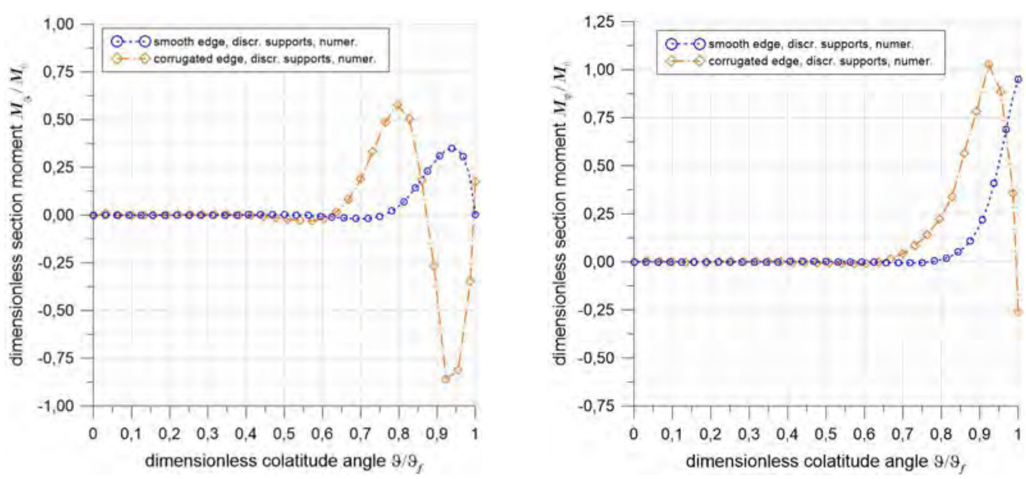

Figure 18: Section moments M_ϑ (left) and M_φ (right) along a meridian located between two supports, i.e. corresponding to the crest of the wave.

It can be pointed out the significant decrease, along the meridian direction, of the bending moment in the corrugated shell, in comparison with the non-corrugated one. That is the most relevant issue. Indeed corrugation, due to its shape, allows for a significant reduction of the bending moment: close to the edge M_ϑ exhibits a noteworthy reduction involving even an inversion of its signum. This improvement can be clearly perceived as a consequence of the stiffness enhancement, which not only depends on the thickness of the shell but also on its shape, i.e. on the presence of a wavy edge. Therefore, edge corrugation enhances the mechanical performance of the shell, without increasing its thickness. On the other hand, M_φ is not similarly subjected to a significant decrease since the surface is essentially warped in the φ direction. Nonetheless, from the point of view of the designer, this difference of behaviour in terms of bending moments has little significance, since for RC shells the standard design rules suggest to adopt symmetric steel bar reinforcement along both ϑ and φ directions.

6. Conclusion

The parametric equations for a shell whose edge is corrugated have been proposed and a suitable FE simulation procedure, which accurately handles the doubly curved geometry, has been presented.

It has been shown through numerical simulation what was intuitively clear to P.L. Nervi: a corrugation along the edge enhances the structural performance of a shell. Furthermore, corrugation considerably decreases the bending moment produced by discrete supports along the shell edge. Indeed, although the shell is designed to behave as a perfect membrane, it can be affected by significant bending on its edge. A reliable procedure has been introduced to study the influence of corrugation into the above-mentioned structures and to evaluate their stress distribution.

The original architectural function related to P.L. Nervi's work, which represents the inspiration for the present paper, has been developed in the sense of Civil and Structural Engineering: corrugated shell structures can be both simply used as a canopy endowed also with some aesthetics, and can be introduced in buildings for their high-performance mechanical properties, like in the case of roofs for special and nuclear waste containers. In this case, a unique shallow shell element must cover the vessel.

Other applications can be found in the field of automatization of building processes. The procedure, which has been presented in this paper, may be applied to different shapes, such as free-form shells and concrete printed structures. Some improvements could be achieved in the LIDAR (Laser Imaging Detection And Ranging) field to accurately identify the influence of small deviation in the structural behaviour; a comparison between a theoretical shape and *in situ* surveys could be done, see for instance [58]. A main issue, which is related to the topic discussed in the present work, will be developed in the following investigations and involves the role of corrugation in instability phenomena, such as snap-through. At this stage, it was intended indeed to highlight the statical intuition envisioned by P.L. Nervi. In this preliminary paper the effect of edge-corrugation is assessed only through linear elastic stress analysis. Under this point of view, corrugation is not an imperfection but is devised in such a way as to improve the structural performance. In a forthcoming paper, buckling will be explicitly addressed and, for this purpose, it will be necessary to take into consideration imperfections in order to trigger the instability phenomena [59–61]. Indeed, the effect of increasing bending stiffness in the spherical shell with respect to buckling problems has been already addressed in the literature [62]. It constitutes however a very challenging problem, whose solution has not been achieved yet.

The methods developed in this paper for Civil Engineering and Architecture applications can be simply generalized to be used in different scientific milieux. One can, for example, use them in the field of Bioengineering for designing new smart contact lenses. This will be the topic of a future development. Moreover, the presented study can be completed and enhanced by taking into account results originally developed for the so-called generalized theories: many interesting phenomena may arise if one introduces higher gradient models like in [63–67].

Numerics play a fundamental role in the solution of problems like that presented in this article: different numerical methods can help in studying different phenomena and they could be implemented also in the study of corrugated shells. One might refer to [68–73] for a detailed discussion.

7. Declaration of competing interest

The authors declare that they have no known competing financial interests or personal relationships that could have appeared to influence the work reported in this paper.

8. Acknowledgements

The authors are grateful to Ph.D. Daniel Meloni for his valuable advice about the use of FE software. The authors are grateful to Prof. Victor Eremeyev for fruitful discussions.

This research has been developed for the partial fulfillment of the doctoral program of M. Lai at *Scuola di Dottorato in Ingegneria Civile e Architettura, University of Cagliari*. It was also carried out under the financial grant of *Place-Doc Exchange Agreement* between the University of Cagliari and the University of Stuttgart, Institute for Non-linear Mechanics, under the supervision of Dr. S.R. Eugster.

The financial support of Fondazione di Sardegna through grant *Surveying, modelling, monitoring and rehabilitation of masonry vaults and domes* i.e. *Rilievo, modellazione, monitoraggio e risanamento di volte e cupole in muratura (RMMR)* (CUP code: F72F20000320007) is grateful acknowledged by M. Lai, E. Reccia, A. Cazzani.

M. Spagnuolo was supported by P.O.R. Sardegna F.S.E. 2014–2020 *Asse III: Istruzione e Formazione, Obiettivo Tematico: 10, Obiettivo Specifico: 10.5, Azione dell'accordo di Partenariato:10.5.12 — Avviso di chiamata per il finanziamento di Progetti di ricerca, Anno 2017*; this support is gratefully acknowledged, too.

References

[1] J. O'Neill, "Walls in half-circles and serpentine walls", *Garden History*, vol. 8, no. 3, pp. 69–76, 1980.

[2] I. Giorgio, U. Andreaus, and A. Madeo, "The influence of different loads on the remodeling process of a bone and bioresorbable material mixture with voids", *Continuum Mechanics and Thermodynamics*, vol. 28, pp. 21–40, 2016.

[3] I. Giorgio, F. dell'Isola, U. Andreaus, F. Alzahrani, T. Hayat, and T. Lekszycki, "On mechanically driven biological stimulus for bone remodeling as a diffusive phenomenon", *Biomechanics and Modeling in Mechanobiology*, vol. 18, pp. 1639–1663, 2019.

[4] Y. Lu and T. Lekszycki, "New description of gradual substitution of graft by bone tissue including biomechanical and structural effects, nutrients supply and consumption", *Continuum Mechanics and Thermodynamics*, vol. 30, pp. 995–1009, 2018.

[5] B. Desmorat and R. Desmorat, "Topology optimization in damage governed low cycle fatigue", *Comptes Rendus Mécanique*, vol. 336, pp. 448–453, 2008.

[6] I. Giorgio and D. Scerrato, "Multi-scale concrete model with rate-dependent internal friction", *European Journal of Environmental and Civil Engineering*, vol. 21, pp. 821–839, 2017.

[7] D. Scerrato, I. Giorgio, A. Madeo, A. Limam, and F. Darve, "A simple non-linear model for internal friction in modified concrete", *International Journal of Engineering Science*, vol. 80, pp. 136–152, 2014.

[8] D. Scerrato, I. Giorgio, A. della Corte, A. Madeo, N. Dowling, and F. Darve, "Towards the design of an enriched concrete with enhanced dissipation performances", *Cement and Concrete Research*, vol. 84, pp. 48–61, 2016.

[9] F. Stochino, M. L. Fadda, and F. Mistretta, "Low cost condition assess-

ment method for existing RC bridges", *Engineering Failure Analysis*, vol. 86, pp. 56–71, 2018.

[10] M. Coni, F. Mistretta, F. Stochino, J. Rombi, M. Sassu, and M. L. Puppio, "Fast falling weight deflectometer method for condition assessment of RC bridges", *Applied Sciences*, vol. 11, pp. 1743–1–18, 2021.

[11] F. Mistretta, G. Sanna, F. Stochino, and G. Vacca, "Structure from motion point clouds for structural monitoring", *Remote Sensing*, vol. 11, pp. 1940–1–20, 2019.

[12] F. Stochino and F. Lopez Gayarre, "Reinforced concrete slab optimization with simulated annealing", *Applied Sciences*, vol. 9, pp. 3161–1–14, 2019.

[13] E. Torroja, "Razón y ser de los tipos estructurales", tech. rep., Consejo Superior de Investigaciones Científicas, Instituto de Ciencias de la Construcción "Eduardo Torroja", Madrid, 2000.

[14] C. Siegel, *Structure and form in modern architecture.* New York: Reinhold, 1966.

[15] G. Pizzetti and A. M. Zorno Trisciuoglio, *Principi statici e forme strutturali.* Torino: Utet, 1980.

[16] T. Iori and S. Poretti, *SIXXI. Storia dell'ingegneria strutturale in Italia*, vol. 1-5. Roma: Gangemi, 2014.

[17] P. L. Nervi, *Scienza o arte del costruire? Caratteristiche e possibilità del cemento armato.* Milano: CittàStudi, 2014.

[18] P. Solomita, *Pier Luigi Nervi vaulted architecture: towards new structures*. Bologna: Bononia University Press, 2015.

[19] T. Leslie, "Carpenter's parametrics: economics, efficiency, and form in Pier Luigi Nervi's concrete designs", *Journal of the International Association for Shell and Spatial Structures*, vol. 54, pp. 107–115, 2013.

[20] E. Tomei, "The Iris Dome", *L'Arca*, vol. 73, pp. 55–57, 1993.

[21] C. A. B. Hyeng and S. N. Krivoshapko, "Umbrella-type surfaces in architecture of spatial structures", *IOSR Journal of Engineering*, vol. 3, no. 3, pp. 43–53, 2013.

[22] S. N. Krivoshapko and V. N. Ivanov, *Encyclopedia of analytical surfaces*. Cham: Springer, 2015.

[23] S. Malek and C. Williams, "The equilibrium of corrugated plates and shells", *Nexus Network Journal*, vol. 19, pp. 619–627, 2017.

[24] A. Norman, S. Guest, and K. Seffen, "Novel multistable corrugated structures", in *48th AIAA/ASME/ASCE/AHS/ASC Structures, Structural Dynamics, and Materials Conference*, pp. 2228–1–12, 2007.

[25] T. Michiels, S. Adriaenssens, and M. Dejong, "Form finding of corrugated shell structures for seismic design and validation using non-linear pushover analysis", *Engineering Structures*, vol. 181, pp. 362–373, 2019.

[26] H. Altenbach and V. A. Eremeyev, *Shell-like structures: Non-classical theories and applications*. Berlin: Springer, 2011.

[27] H. Altenbach and V. A. Eremeyev, “On the shell theory on the nanoscale with surface stresses”, *International Journal of Engineering Science*, vol. 49, pp. 1294–1301, 2011.

[28] J. Altenbach, H. Altenbach, and V. A. Eremeyev, “On generalized Cosserat-type theories of plates and shells: a short review and bibliography”, *Archive of Applied Mechanics*, vol. 80, pp. 73–92, 2010.

[29] V. A. Eremeyev, “Two- and three-dimensional elastic networks with rigid junctions: modeling within the theory of micropolar shells and solids”, *Acta Mechanica*, vol. 230, pp. 3875–3887, 2019.

[30] V. Eremeyev and H. Altenbach, “Basics of mechanics of micropolar shells”, in *Shell-like Structures* (H. Altenbach and V. Eremeyev, eds.), pp. 63–111, Cham: Springer, 2017.

[31] J. Chróścielewski, F. dell’Isola, V. A. Eremeyev, and A. Sabik, “On rotational instability within the nonlinear six-parameter shell theory”, *International Journal of Solids and Structures*, vol. 196-197, pp. 179–189, 2020.

[32] V. A. Eremeyev, “A nonlinear model of a mesh shell”, *Mechanics of Solids*, vol. 53, pp. 464–469, 2018.

[33] A. M. Bersani, I. Giorgio, and G. Tomassetti, “Buckling of an elastic hemispherical shell with an obstacle”, *Continuum Mechanics and Thermodynamics*, vol. 25, pp. 443–467, 2013.

[34] L. Greco and M. Cuomo, “An implicit G^1-conforming bi-cubic interpolation for the analysis of smooth and folded Kirchhoff–Love shell as-

semblies", *Computer Methods in Applied Mechanics and Engineering*, vol. 373, pp. 113476–1–45, 2021.

[35] Z.-T. Chang, M. A. Bradford, and R. Ian Gilbert, "Limit analysis of local failure in shallow spherical concrete caps subjected to uniform radial pressure", *Thin-Walled Structures*, vol. 48, no. 6, pp. 373–378, 2010.

[36] Z.-T. Chang, M. A. Bradford, and R. I. Gilbert, "Short-term behaviour of shallow thin-walled concrete dome under uniform external pressure", *Thin-Walled Structures*, vol. 49, pp. 112–120, 2011.

[37] A. Zingoni, "Liquid-containment shells of revolution: A review of recent studies on strength, stability and dynamics", *Thin-Walled Structures*, vol. 87, pp. 102–114, 2015.

[38] C. Maraveas, G. A. Balokas, and K. D. Tsavdaridis, "Numerical evaluation on shell buckling of empty thin-walled steel tanks under wind load according to current American and European design codes", *Thin-Walled Structures*, vol. 95, pp. 152–160, 2015.

[39] A. Niloufari, H. Showkati, M. Maali, and S. Mahdi Fatemi, "Experimental investigation on the effect of geometric imperfections on the buckling and post-buckling behavior of steel tanks under hydrostatic pressure", *Thin-Walled Structures*, vol. 74, pp. 59–69, 2014.

[40] E. Verwimp, T. Tysmans, M. Mollaert, and S. Berg, "Experimental and numerical buckling analysis of a thin TRC dome", *Thin-Walled Structures*, vol. 94, pp. 89–97, 2015.

[41] E. Verwimp, T. Tysmans, M. Mollaert, and M. Wozniak, “Prediction of the buckling behaviour of thin cement composite shells: Parameter study”, *Thin-Walled Structures*, vol. 108, pp. 20–29, 2016.

[42] D. Zou, J. Sun, H. Wu, Y. Hao, Z. Wang, and L. Cui, “Experimental and numerical studies on the impact resistance of large-scale liquefied natural gas (LNG) storage outer tank against the accidental missile”, *Thin-Walled Structures*, vol. 158, pp. 107189–1–18, 2021.

[43] F. L. Jiménez, J. Marthelot, A. Lee, J. W. Hutchinson, and P. M. Reis, “Technical brief: knockdown factor for the buckling of spherical shells containing large-amplitude geometric defects”, *ASME Journal of Applied Mechanics*, vol. 84, pp. 034501–1–4, 2017.

[44] E. Turco and N. L. Rizzi, “Pantographic structures presenting statistically distributed defects: Numerical investigations of the effects on deformation fields”, *Mechanics Research Communications*, vol. 77, pp. 65–69, 2016.

[45] Y. Solyaev, S. Lurie, E. Barchiesi, and L. Placidi, “On the dependence of standard and gradient elastic material constants on a field of defects”, *Mathematics and Mechanics of Solids*, vol. 25, pp. 35–45, 2020.

[46] L. Placidi, E. Barchiesi, and A. Misra, “A strain gradient variational approach to damage: a comparison with damage gradient models and numerical results”, *Mathematics and Mechanics of Complex Systems*, vol. 6, pp. 77–100, 2018.

[47] L. Placidi and E. Barchiesi, "Energy approach to brittle fracture in strain-gradient modelling", *Proceedings of the Royal Society A: Mathematical, Physical and Engineering Sciences*, vol. 474, pp. 20170878–1–19, 2018.

[48] U. Mühlich, "Deformation and failure onset of random elastic beam networks generated from the same type of random graph", in *Developments and Novel Approaches in Biomechanics and Metamaterials* (B. E. Abali and I. Giorgio, eds.), pp. 393–408, Cham: Springer, 2020.

[49] I. Bucur-Horváth and R. V. Săplăcan, "Force lines embodied in the building: Palazzetto dello sport", *Journal of the International Association for Shell and Spatial Structures*, vol. 54, pp. 179–187, 2013.

[50] P. di Re, E. Lofrano, J. Ciambella, and F. Romeo, "Structural analysis and health monitoring of twentieth-century cultural heritage: the Flaminio Stadium in Rome", *Smart Structures and Systems*, vol. 27, pp. 285–303, 2021.

[51] V. G. Rekach, *Static theory of thin-walled space structures.* Moscow: Mir, 1978.

[52] W. Flügge, *Stresses in shells.* Berlin: Springer, 1960.

[53] S. P. Timoshenko and S. Woinowsky-Krieger, *Theory of plates and shells.* New York: McGraw-Hill, 2nd ed., 1959.

[54] D. P. Billington, *Thin shell concrete structures.* New York: McGraw-Hill, 1965.

[55] V. Gioncu, *Thin reinforced concrete shells: special analysis problems*. Bucarest: Wiley, 1979.

[56] A. M. Haas, *Thin concrete shells*, vol. 1. New York: Wiley, 1962.

[57] A. M. Haas, *Thin concrete shells*, vol. 2. New York: Wiley, 1967.

[58] R. Argiolas, A. Cazzani, E. Reccia, and V. Bagnolo, "From LIDAR data towards HBIM for structural evaluation", *The International Archives of the Photogrammetry, Remote Sensing and Spatial Information Sciences*, vol. XLII-2/W15, pp. 125–132, 2019.

[59] H. Wagner, C. Hühne, and S. Niemann, "Robust knockdown factors for the design of spherical shells under external pressure: Development and validation", *International Journal of Mechanical Sciences*, vol. 141, pp. 58–77, 2018.

[60] H. Wagner, C. Hühne, J. Zhang, W. Tang, and R. Khakimova, "Geometric imperfection and lower-bound analysis of spherical shells under external pressure", *Thin-Walled Structures*, vol. 143, pp. 106195–1–13, 2019.

[61] H. Wagner, C. Hühne, J. Zhang, and W. Tang, "On the imperfection sensitivity and design of spherical domes under external pressure", *International Journal of Pressure Vessels and Piping*, vol. 179, pp. 104015–1–12, 2020.

[62] T. von Kármán and H.-S. Tsien, "The Buckling of spherical shells by external pressure", *Journal of the Aeronautical Sciences*, vol. 7, pp. 43–50, 1939.

[63] V. A. Eremeyev and F. dell'Isola, "On weak solutions of the boundary value problem within linear dilatational strain gradient elasticity for polyhedral Lipschitz domains", *Mathematics and Mechanics of Solids*, 2021. DOI: 10.1177/10812865211025576.

[64] J.-J. Alibert, P. Seppecher, and F. dell'Isola, "Truss modular beams with deformation energy depending on higher displacement gradients", *Mathematics and Mechanics of Solids*, vol. 8, pp. 51–73, 2003.

[65] F. dell'Isola, P. Seppecher, and A. della Corte, "The postulations *á la D'Alembert* and *á la Cauchy* for higher gradient continuum theories are equivalent: a review of existing results", *Proceedings of the Royal Society A: Mathematical, Physical and Engineering Sciences*, vol. 471, pp. 20150415–1–25, 2015.

[66] P. Seppecher, J.-J. Alibert, and F. dell'Isola, "Linear elastic trusses leading to continua with exotic mechanical interactions", *Journal of Physics: Conference Series*, vol. 319, pp. 012018–1–13, 2011.

[67] V. A. Eremeyev, A. Cazzani, and F. dell'Isola, "On nonlinear dilatational strain gradient elasticity", *Continuum Mechanics and Thermodynamics*, vol. 33, pp. 1429–1463, 2021.

[68] F.-F. Wang, H.-H. Dai, and I. Giorgio, "A numerical comparison of the uniformly valid asymptotic plate equations with a 3D model: Clamped rectangular incompressible elastic plates", *Mathematics and Mechanics of Solids*, 2021. DOI: 10.1177/10812865211025583.

[69] L. Greco and M. Cuomo, "B-Spline interpolation of Kirchhoff-Love space rods", *Computer Methods in Applied Mechanics and Engineering*, vol. 256, pp. 251–269, 2013.

[70] M. Cuomo, L. Contrafatto, and L. Greco, "A variational model based on isogeometric interpolation for the analysis of cracked bodies", *International Journal of Engineering Science*, vol. 80, pp. 173–188, 2014.

[71] L. Greco, M. Cuomo, and L. Contrafatto, "A reconstructed local B formulation for isogeometric Kirchhoff–Love shells", *Computer Methods in Applied Mechanics and Engineering*, vol. 332, pp. 462–487, 2018.

[72] M. E. Yildizdag, M. Demirtas, and A. Ergin, "Multipatch discontinuous Galerkin isogeometric analysis of composite laminates", *Continuum Mechanics and Thermodynamics*, vol. 32, pp. 607–620, 2020.

[73] C. Olivieri, M. Angelillo, A. Gesualdo, A. Iannuzzo, and A. Fortunato, "Parametric design of purely compressed shells", *Mechanics of Materials*, vol. 155, pp. 103782–1–10, 2021.